Measurement 265 (2026) 120269

Contents lists available at ScienceDirect

Measurement

journal homepage: www.elsevier.com/locate/measurement

Cavitation modelling and ML integration in the DT prediction of extreme pressure heads

Oscar E. Coronado-Hernández [a], Duban A. Paternica-Verona [b], Modesto Pérez-Sánchez [c,*], Dídia I.C. Covas [d], Helena M. Ramos [d,*]

[a] Instituto de Hidráulica y Saneamiento Ambiental, Universidad de Cartagena, Cartagena 130001, Colombia
[b] School of Civil Engineering Universidad del Sinú, Cartagena 130014, Colombia
[c] Hydraulic Engineering and Environmental Department, Universitat Politècnica de València, 46022 Valencia, Spain
[d] CERIS member, Instituto Superior Técnico, Universidade de Lisboa 1049-001 Lisboa, Portugal

ARTICLE INFO

Keywords:
Cavitation modelling
Pipe systems
Air-valve
Pressure transients
Multiphase flow
Machine Learning

ABSTRACT

This research presents a hybrid approach exemplifying the convergence of deterministic modelling and data-driven prediction to enhance simulation fidelity in complex hydraulic systems. It integrates experimental testing, numerical modelling, and Machine Learning (ML) to analyse hydraulic transients and cavitation. Laboratory water hammer tests validated simulations using a developed Cavitation Model (CM) and an adapted Bentley's Hammer, both based on the 1D Method of Characteristics (MOC) with discrete cavity representation when vapour pressure is reached. Comparisons between experimental data and CM outputs provided insights into Digital Twin (DT) applications. Air valve behaviour was also highlighted, as improper integration can destabilise transient flows in slightly sloped profiles. In parallel, an ML framework was developed to predict maximum (Hmax) and minimum (Hmin) pressure heads from flow rates (25–950 l/h) and pipe diameters (0.005–0.06 m). Using 5-fold cross-validation with 35 % of data reserved for testing, a three-layer neural network achieved R^2 values of 0.86 (Hmax) and 0.94 (Hmin) in validation, and 0.46 (Hmax) and 0.91 (Hmin) in testing. The strong alignment between predicted and simulated/measured values, particularly demonstrates the integrated model's value in identifying cavitation risks and enabling proactive system management and design optimisation without reliance on complex hydraulic simulations.

1. Introduction

The literature addressing cavitation and hydraulic transients has evolved significantly, integrating both classical modelling approaches and modern machine learning techniques [1]. provide a foundational historical review of water hammer phenomena with column separation, emphasising the challenges in modelling vapour cavity formation and collapse in pressurised systems. Their work laid the groundwork for understanding the dynamics of transient cavitation in fluid transport networks [1]. Building on this fundamental, [2] explored the dynamic effects of transient flows with cavitation in pipe systems through experimental and numerical studies. Presented at the 9th International Conference on Pressure Surges, their research highlighted the role of air valves and boundary conditions in mitigating pressure surges and cavitation onset [2]. The authors further contributed to this domain by combining modelling and experimental validation to analyse surge damping mechanisms. Their study demonstrated how air valves can effectively control pressure transients and reduce cavitation risks in pipeline systems [3]. Recent advances have introduced machine learning into this field, offering new tools for reconstructing and predicting cavitation behaviour. Cheng et al. (2024) developed a deep learning framework for data assimilation in fluid systems with sparse and time-varying sensor inputs. Although not cavitation-specific, their approach provides scalable ML techniques for reconstructing transient flow fields, which are highly relevant to hydraulic modelling [4]. [5] used a combined clustering and regularised neural network to analyse the burst detection, localisation and flow/pressure sensor placement in water distribution networks. Li et al. (2024) extended this line of inquiry by proposing an improved deep learning model for sparse reconstruction of cavitation flow fields. Using transformer-based architectures, their model enhances prediction accuracy and convergence speed, offering a powerful tool for analysing cavitating flows in complex systems [6]. Ref [7] synthesised experimental and numerical insights into two-phase flow dynamics, including pressure surges, cavitation, and ventilation,

* Corresponding authors.

https://doi.org/10.1016/j.measurement.2025.120269
Received 30 October 2025; Received in revised form 23 December 2025; Accepted 30 December 2025
Available online 9 January 2026

highlighting the interplay between air valve behaviour and transient flow interactions. Complementary studies examined the effect of commercial air valves on rapid pipeline filling and developed real-time Digital Twin modelling for CFD-based valve control [8,9]. Together, these works illustrate the progression from classical hydraulic modelling to data-driven approaches, underscoring the importance of integrating experimental validation, numerical simulation, and machine learning in understanding cavitation in hydraulic transients.

Pipeline buckling collapse is a critical failure mode that arises when internal pressure drops below atmospheric levels during transients such as valve closures or pump shutdowns. Cavitation intensifies this risk by generating vapour cavities that collapse violently, producing shock waves and destabilising pipe structures [10]. Air valves are essential to mitigate these effects, as they prevent vacuum conditions by admitting atmospheric air during depressurisation and expel trapped air during pressurisation [11,12]. Their strategic placement at high points or along long horizontal sections ensures continuous venting, stabilises internal pressure, and protects against collapse [7]. Proper venting also avoids compressible air pockets that could amplify surges and structural stress [13,14]. Without functioning air valves, negative pressure events can lead to severe deformation or collapse (Fig. 1a), making their integration a fundamental design practice for safety, structural integrity, and mitigation of cavitation and transient pressure drops [15] (Fig. 1b).The operational effectiveness of air-valves contributes significantly to: System Protection (Fig. 1c): By eliminating air pockets, they reduce the risk of pressure surges and water hammer events; Energy Efficiency: Maintaining air-free flow minimises head loss and improves pump performance; Preventive Maintenance: Regular air expulsion prevents corrosion in pipe crowns and maintains measurement accuracy in flow meters.

Proper selection and installation require careful consideration of system pressure ratings, flow conditions, and the specific air handling capacity needed for optimal performance in different pipeline configurations [89].

Active protection systems rely on real-time monitoring networks with pressure transducers and flow meters, supported by Digital Twin (DT) technologies [16] and automated response algorithms that trigger protective devices within milliseconds, as well as predictive control systems using machine learning to anticipate transient events. Passive protection systems, in contrast, include hydraulic capacitors such as surge tanks with optimised gas–liquid ratios, hydropneumatic tanks, wave reflection techniques achieved by strategic pipe diameter changes, and energy dissipation devices based on orifice plates and diffusers. Emerging security technologies further enhance hydraulic system protection, incorporating smart surge mitigation, IoT-enabled valves with adaptive response profiles, distributed acoustic sensing for early transient detection, blockchain-based maintenance logs for surge protection devices, advanced materials such as self-healing pipe coatings and nanocomposites with improved fatigue resistance, and hybrid protection systems that combine mechanical and electronic surge arrestors, hydraulic dampers with tuneable characteristics, and AI-optimised protection device networks [56]. However, security standards and compliance use modern hydraulic systems to meet increasingly stringent security requirements, such as International Standards of type AWWA M51 (American Water Works Association) [15] for water hammer control, ISO 21839 (International Organization for Standardization). For hydraulic transient analysis, the European Norm (EN 805) for water supply system security, and certification protocols for surge protection device performance testing, system resilience certification, cybersecurity for Supervisory Control and Data Acquisition controlled (SCADA) surge systems, and regulatory requirements present mandatory transient analysis for critical infrastructure and periodic surge protection system inspections and failure reporting and analysis documentation [17]. There is still a need for more accurate, integrated and more complete analytical models.

2. Methodology

The methodology integrates classical hydraulic modelling with modern predictive approaches by combining the Method of Characteristics (MOC) with a cavitation model. MOC, a well-established numerical tool for transient flow in pressurised systems, solves the governing equations of unsteady flow through pipeline discretisation and boundary condition definition. Within this framework, a tailored cavitation model is incorporated to capture system behaviour under cavitation effects. A cavitation model catalogues all critical physical elements of the pipeline system: (i) Pipes: length (L), internal diameter (D), and material, which determines elastic wave speed; (ii) Valves: locations and closure characteristics (Tc = time to fully close, closure rate function); (iii) Pumps/Turbines: includes performance curves (H-Q relationships) and trip/shutdown profiles; (iv) Cavitation Model: selects appropriate vapor cavity formation criteria based on fluid vapor pressure. This accounts for situations where the pressure head, H, drops below the vapour pressure head, *H*vap. If cavitation occurs, the model imposes H=Hvap and sets the vapour cavity formation. Otherwise, the standard governing equations are applied (Continuity and Momentum equations). To ensure accuracy, a Courant condition is used and a governing time-step stability.

Fig. 2 presents a structured computational framework for modelling fluid transients in pipelines, with a particular focus on cavitation and pressure wave propagation. It integrates classical hydraulic equations—continuity and momentum—with numerical techniques such as the Method of Characteristics (MOC), discretization schemes, and boundary condition formulations. Cavitation is addressed through conditional logic that enforces vapor pressure constraints. The model also incorporates the Courant condition for numerical stability and pump behaviour via head–flow relationships. A machine learning (ML) module is embedded to predict maximum and minimum pressure heads (Hmax and Hmin) based on diameter (D) and flow rate (Q), guiding the selection of the optimal solution. This hybrid approach exemplifies the convergence of deterministic modelling and data-driven prediction to enhance simulation fidelity in complex hydraulic systems. Finally, the

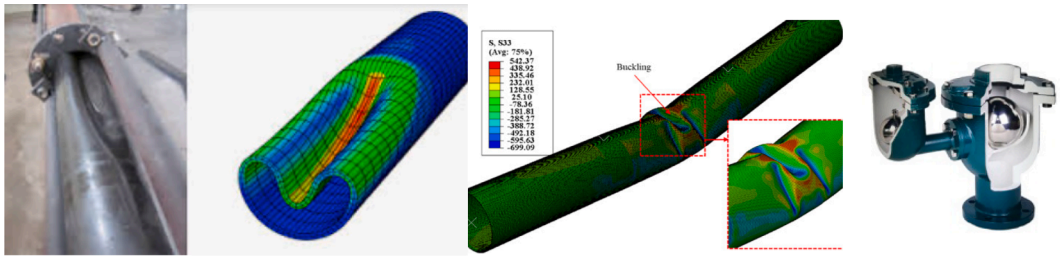

Fig. 1. Buckling collapse of a pipe and typical air-valve protection device. (a) Photo; (b) CFD simulation; (c) Air valve.

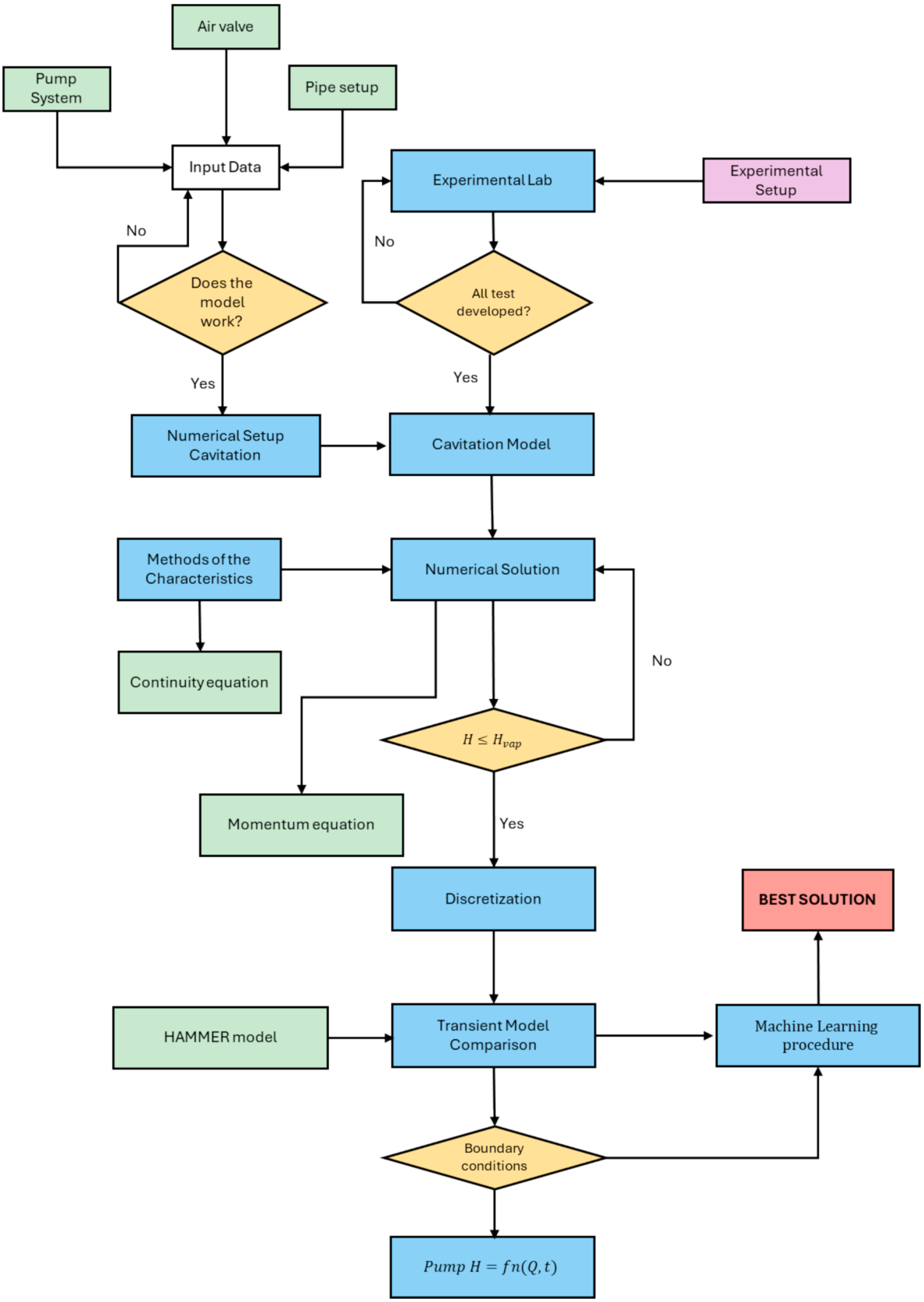

Fig. 2. Brief methodology for the specific transient model with cavitation and ML prediction.

methodology integrates Machine Learning (ML) [10,18,19], where the ML model predicts maximum and minimum heads (Hmax and Hmin) for given flow and pipe diameter conditions (D, Q). This allows for getting the best solution with a rapid estimation of extreme transient responses without requiring a full simulation each time. The methodology combines a physics-based experimental transient flow solver with a mathematical model (i.e., MOC with cavitation modelling) and a data-driven ML layer (Fig. 2). This hybrid framework reduces computational effort by guiding solutions without full simulations, while leveraging the accuracy of numerical models and the speed of ML to efficiently evaluate transient pressures and support optimal design and operation decisions.

2.1. Numerical setup of cavitation and air-valves modelling

The simulated systems are composed of a uniform transmission pipeline with a reservoir and a sectioning valve at the downstream end. The numerical gridline is chosen to satisfy the Courant-Friedrichs-Lewy (CFL) stability condition:

$$C_R = \frac{c}{\frac{\Delta x}{\Delta t}} \leq 1 \tag{1}$$

where Cr = Courant number; c = wave speed; Δt = numerical time increment; Δx = numerical space increment.

For modelling purposes, the effect of air release is neglected, and discrete vapour cavities can open at all pipe sections. Hence, macro cavitation (large cavities) can be characterised by the existence of a vapour cavity volume $\forall_{i,j}$ at the pipe section i and for the time j as follows:

$$\forall_{i,j} = \forall_{i,j-1} + \frac{(Q_{Ri,j} + Q_{Ri,j-1} - Q_{Li,j} - Q_{Li,j-1})\Delta t}{2} \tag{2}$$

where Q_R and Q_L is the discharge at the right and the left side of the cavity, respectively.

This condition is imposed when the absolute pressure drops to the liquid vapour pressure (vaporous cavitation inception) H_{IC} (ca. −8 to −10 m depending on the site conditions), and maintains this value if the cavity volume is positive. The piezometric head within the cavity is given by:

$$H_\forall = H_{IC} + \frac{p_{atm}}{\gamma} \tag{3}$$

The application of the MOC to the typical "reservoir-pipe-valve" allows the definition of the main equations. For a reservoir with a constant water level (Z):

$$H_P = Z \tag{4}$$

when solved simultaneously with the characteristic line C^- it allows the calculation of Q_P (by using a first-order integration),

$$Q_P = \frac{Z - C_2}{B} \tag{5}$$

with $B = \frac{c}{gS}$ and c the wave speed.

For an intermediate pipe section, characteristic lines C^+ and C^- must be used and if the air volume inside the pipe is null (i.e., $\forall = 0$), then

$$H_R - H_L + 2BQ_P - B(Q_R + Q_L) + R(|Q_L|Q_L + |Q_R|Q_R) = 0 \tag{6}$$

yielding for Q_P,

$$Q_P = \frac{C_1 - C_2}{2B} \tag{7}$$

$$H_P = \frac{C_1 + C_2}{2} \tag{8}$$

when $H_P \leq H_{\forall ap}$ then the head and flow are calculated according to Eqs. (9) and (10),

$$H_P - H_A + Q_{PL} - Q_A + R|Q_{PL}|Q_{PL} = 0 \tag{9}$$

Solving results in

$$Q_{PL} = \frac{2(Q_A + H_A - H_P)}{1 + \sqrt{1 + 4R|Q_A + H_A - H_P|}} \tag{10}$$

and the same to the right side of the cavity:

$$Q_{PD} = \frac{2(Q_B - H_B + H_P)}{1 + \sqrt{1 + 4R|Q_B - H_B + H_P|}} \tag{11}$$

At the valve section, with a quasi-instantaneous discharge reduction and if the cavity volume is$\forall = 0$ then QP = 0 and based on C+:

$$H_P = H_L + (B - R|Q_L|)Q_L \tag{12}$$

but if HP < $H_\forall$then

$$Q_P = \frac{C_1 - H_\forall}{B} \tag{13}$$

and

$$\forall_2 = \forall_1 + (Q_P - Q_L)\ \Delta t \tag{14}$$

In the calculus, if$\forall < 0$ then is considered$\forall = 0$ and the procedures is repeated.

On the other hand, the importance of air valves to avoid the buckling effect associated with cavitation can be stated as:

Continuity equation for the air

$$\forall_{air} = \forall_{air} - \Delta t(Q_{PL} - Q_{PR}) \tag{15}$$

with ∀air, the air volume inside the pipe, and Q_{PL}, Q_{PR}, the discharge at the left/right system section, respectively. When the valve is opened, the following equation is valid (16).

$$H_P = Z_V \tag{16}$$

where H_P is the piezometric head at any section of the conveyance system and Z_V is the head at the valve location.

If the air valve is closed with air inside, then Eq. (17) is used

$$H_P - Z_V + 10.3 = \frac{K_\forall}{\forall_{AR}} \tag{17}$$

The percentage of air that is contained in the flow is assumed to have an isothermal (n = 1) behaviour, which is translated into

$$H\forall_{air}^n = cte \tag{18}$$

However, if the air-valve is closed but without air inside the pipe, then

$$Q_{PM} = Q_{PJ} \tag{19}$$

The following analysis illustrates the variation in system response for an air valve located at the high point of the pipe profile, with different closure times and percentages of retained air inside the pipe due to air drag caused by transient conditions with forward and backwards pressure waves.

2.2. Experimental setup

An experimental rig has been built in the base configuration "reservoir-pipe-valve" (Fig. 3a) and consists of a coiled copper pipe of approximately 100 m in length (figure 3b), with an inside diameter of 20 mm and a wall thickness of 1 mm. Currently, the system is supplied from a 125 L storage tank (figure 3c), which feeds a pump (Fig. 3d), which can be controlled with a valve at the downstream.

Downstream of the pump, there is a hydropneumatic vessel with a capacity of 60 l, in stainless steel and a nominal pressure of 6 bar. At the end, there are two valves, a globe valve with a nominal diameter 15

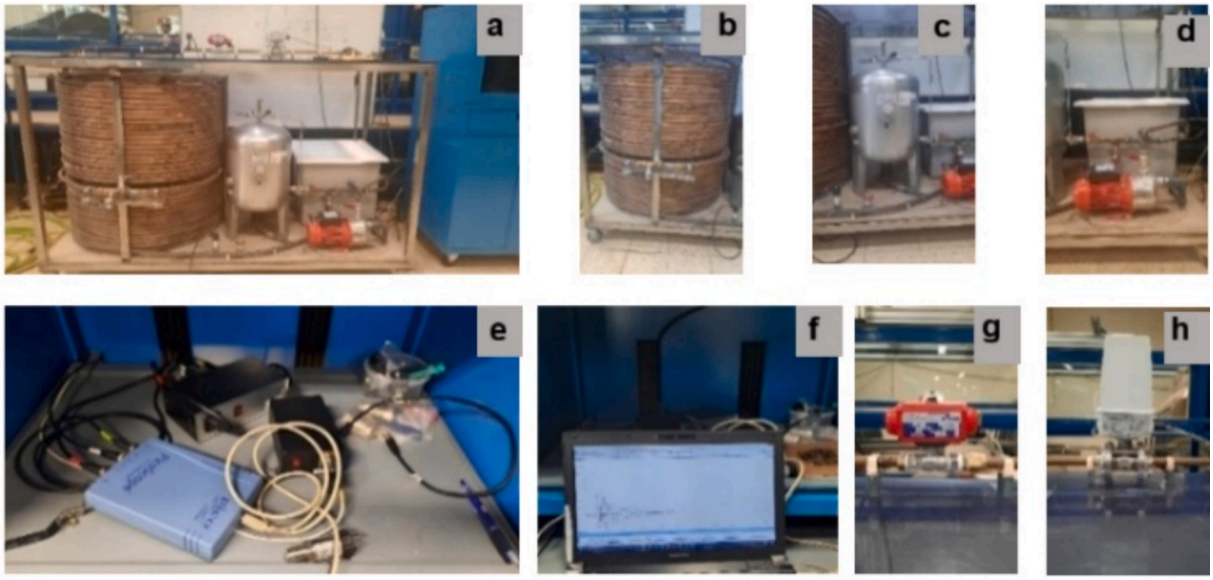

Fig. 3. Experimental setup: (a) system view; (b) coiled copper pipe; (c) hydropneumatic vessel; (d) pump; (e) picoscope for data acquisition; (f) computer; (g) automatic valve; (h) flow meter.

(DN15 1/2) and a ball valve with a DN 3/4 (Fig. 3). The experimental setup was developed to study pressure wave propagation, water hammer, and cavitation in piping systems. It consists of: (a) a hydraulic test rig providing an overall system view; (Fig. 3b) a coiled copper pipe, offering thermal conductivity and corrosion resistance while maximising length in compact space; (Fig. 3c) a pressurised hydropneumatic vessel acting as a surge suppressor to damp pressure fluctuations; (Fig. 3d) a centrifugal pump generating steady flow and pressure; (Fig. 3e) monitoring instruments including a Picoscope, DAQ device, and surge protector to record and safeguard system behaviour; (Fig. 3f) a computer with specialised software (MATLAB, LabVIEW, or custom tools) for data processing, real-time display, and predictive modelling; (Fig. 3g) an automatic hydropneumatic valve enabling controlled opening/closing to induce water hammer events; and (Fig. 3h) a flow meter (turbine, ultrasonic, or electromagnetic) providing accurate measurements of flow rate, integrated into the DAQ system. Together, these components allow detailed analysis of transient pressures, comparison of experimental and theoretical results, and optimisation of hydraulic designs.

3. Results and discussion

3.1. Experiments

To gather the necessary data, experimental tests are conducted at the Hydraulic Laboratory of the Civil Engineering Department of Instituto Superior Técnico. The pump is turned on and the automatic valve is pressurised, as well as other devices such as the picoscope and the data acquisition device, through the power surge equipment. The flow meter measures the required flow for the validation process. For the next step, the automatic valve is instantly closed to create a high-pressure surge across the system.

The data is captured (Fig. 4) in one transducer located downstream, near the automatic valve, and another upstream near the hydropneumatic tank. Fig. 3 illustrates the pressure head in those transducers during the valve closure-induced transient event.

3.2. Transient mathematical models

Both HAMMER and the developed Cavitation Model share a common numerical foundation, employing the one-dimensional Method of Characteristics (1D MOC) with CFL-based time-step control to ensure stability in simulating pressure wave propagation. However, they differ in key operational aspects. HAMMER allows flexible wave-speed input, either user-defined or calculated from fluid and pipe properties, while the Cavitation Model requires explicit user definition, offering greater control but demanding precision. Valve closure behaviour also diverges: HAMMER uses user-defined closure curves, whereas the Cavitation Model applies a coded closure law. Cavitation treatment is simplified in HAMMER through a vapour-cavity flag, while the Cavitation Model

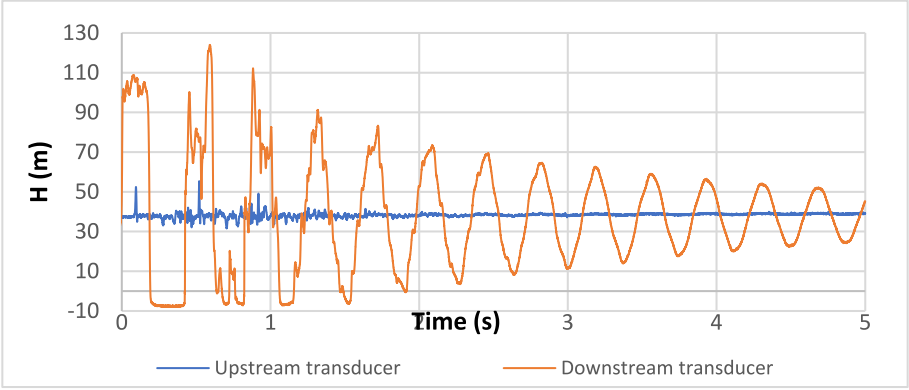

Fig. 4. Experiments in the lab test rig for a transient event of downstream valve closure for an initial flow of 675 l/h.

employs a user-defined algorithm for more detailed analysis. Finally, HAMMER is a commercial, industry-oriented tool with standardised features and user-friendly interfaces, whereas the Cavitation Model is a research-oriented framework designed for customised and transparent cavitation simulation. The Cavitation Model, on the other hand, is a scientific research tool tailored for academic exploration, offering greater flexibility for theoretical development and experimental validation. Together, these comparisons highlight how each model serves distinct purposes while sharing a common computational backbone (Table 1).

3.3. Cavitation model (CM) calibration and comparisons of mathematical models

For the Cavitation Model (CM) calibration, many features of the model were designed to be changed for further modifications and analysis. Parameters such as total length, pipe diameter, wave speed, flow and others could be changed to improve results. In this model, a fixed wave speed value was considered, of 1150 m/s was considered, based on test results.

It is possible to observe that the initial pressure peaks match the ones from the laboratory data, and the dissipation rate fits better in the Cavitation Model. The Cavitation Model also provides a variation showing pressure envelopes, where a maximum and minimum pressure line is exhibited, as well as the pipe profile elevation line. Fig. 5 allows a better understanding of how pressure upsurges or downsurges occur throughout the pipe system length. Upon further modifications of some parameters, the optimised version of the model was considered.

There are some general key observations regarding the cavitation Model with lab experiments: (i) in terms of general agreement both curves exhibit typical behaviour, indicating transient hydraulic phenomena such as water hammer or pressure wave reflections along the pipe system with no other special induced reflection waves. The Cavitation Model closely tracks the Laboratory data, validating its ability to simulate real-world cavitation dynamics, (ii) in terms of amplitude differences, the Laboratory curve shows slightly higher peak amplitude, especially in the early seconds. This suggests the model may slightly underestimate pressure extreme, possibly due to damping assumptions in terms of resistive coefficients; (iii) in the phase shift.

minor phase lag is visible between the two curves, which can be justified due to time discretization in the numerical scheme different from the acquisition frequency, simplified boundary conditions or valve dynamics in the model. The Cavitation Model captures the negative pressure and vapour cavity formation realistically. Regarding the implications for validation, the Cavitation Model demonstrates strong predictive capability, with good alignment in both amplitude and frequency. Slight discrepancies suggest areas for refinement such as incorporating more accurate valve dynamics or boundary conditions, and adjusting damping coefficients or vapor cavity collapse parameters.

In terms of overview of this comparison, in X-axis: Time (s), ranging from 0 to 5 s and Y-axis: Head (H) in meters, ranging from −20 to 160 m, where are observed some key performance indicators: (i) Amplitude and Extremes: HAMMER shows sharp peaks and troughs (Fig. 6), with head values reaching above 150 m and dipping below 0 m, Cavitation Model maintains more moderate oscillations, staying within a narrower head range; (ii) Oscillation Behaviour: HAMMER exhibits high-frequency fluctuations, suggesting a more reactive or less damped transient response, Cavitation Model appears smoother, indicating damping effects likely due to cavitation modelling or energy dissipation mechanisms; (iii) Cavitation Representation: The negative followed by the sharp positive head values in HAMMER suggest more time with vacuum conditions and the Cavitation Model seems more controlled showing a cavitation duration of 1.5 s, incorporating vapour cavity formation and collapse, moderating extremes and the damping effect.

Table 1
Differences and similarities between model characteristics.

Feature	*HAMMER* model	Cavitation model (CM)
Numerical scheme	1D MOC solver	1D MOC solver
Wave-speed input	Calculated from material and fluid characteristics	Defined by the user
Valve closure modelling	User-defined closure and rating curves	Coded closure-profile function
Cavitation treatment	Vapour-cavity flag for a certain pressure threshold	User-defined vapour-cavity algorithm
Time-step control	Automated CFL check	Automated CFL check
Type of model	Commercial model – more complete data input, but more difficult to detect spurious errors	Research model – friendly use and simpler to control anomalies

When comparing the two simulated transient models with the laboratory one, it is possible to observe that HAMMER simulations have sharper pressure peaks along time duration, while those presented in the Cavitation Model appear in a better phase with experiments. Regarding oscillation duration, the *HAMMER* model oscillation presents some spikes and then decays more rapidly when compared to the lab and CM. It is possible to verify that, after the first two pressure peaks, the Cavitation Model curve maintains a constant decay in timing and shape, as observed in lab tests. Table 2 and Fig. 6 present some characteristics of both models, which generally suit the proposal design conditions.

3.4. ML algorithms application

3.4.1. Predictive scope and model architecture and training strategy

The use of water flow rate (Q) and internal pipe diameter (D) as input features reflects a physically grounded approach to modelling hydraulic transients. These variables directly influence wave propagation speed, pressure head amplitude, and cavitation susceptibility, such as:

- Flow Rate (Q): Higher flow rates increase kinetic energy, potentially amplifying pressure surges and transient oscillations.
- Pipe Diameter (D): Smaller diameters intensify velocity gradients and frictional losses, which can exacerbate pressure drops and cavitation onset.

A sensitivity analysis is incorporated to quantify the relative influence of each predictor on Hmax and Hmin. This enhances interpretability and guides feature selection for future models.

The three-layered neural network was employed considering the predictors of D and Q (Fig. 7). The output vector can be computed as follows:

$$\boldsymbol{a}^3 = f^3\left(LW^{3,2} f^2\left(LW^{2,1} f\left(IW^{1,1}\boldsymbol{p} + \boldsymbol{b}^1\right) + \boldsymbol{b}^2\right) + \boldsymbol{b}^3\right) \tag{20}$$

where, $\boldsymbol{p}$ = predictors vector, $\boldsymbol{a}$ = response vector, $\boldsymbol{W}$ = weight matrix, $\boldsymbol{b}$ = bias vector, $\boldsymbol{IW}$ = predictor weight matrix, and $\boldsymbol{LW}$ = layer weight matrix.

The three-layered neural network's success suggests an optimal balance between model complexity and generalisation. Key architectural choices likely include:

- Input Layer: Normalised Q and D values
- Hidden Layers: Nonlinear activation functions to capture complex hydraulic interactions
- Output Layer: Continuous regression outputs for Hmax and Hmin

The 5-fold cross-validation with a 20 % test split ensures robustness against overfitting and provides reliable generalisation metrics. Additional metrics such as RMSE, MAE, and bias can be used to complement the R^2 values (Fig. 7). Simulations were conducted using Matlab R2024b [20].

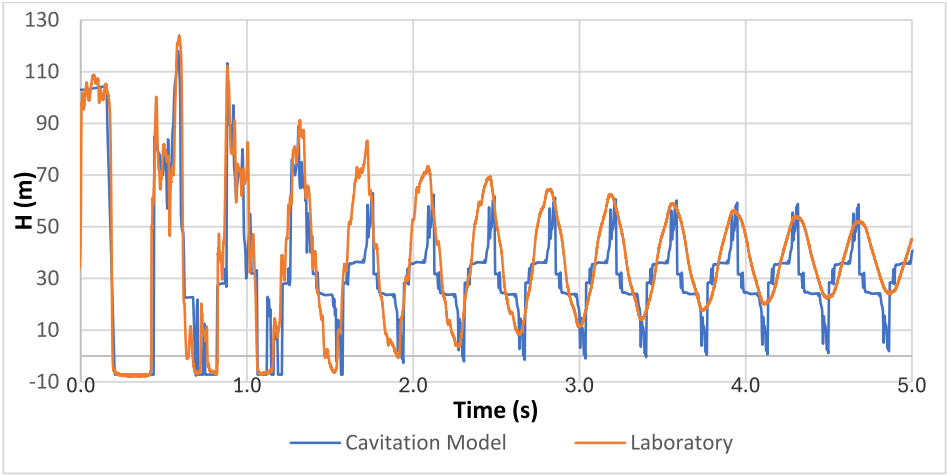

Fig. 5. Example of calibration of the CM based on experiments.

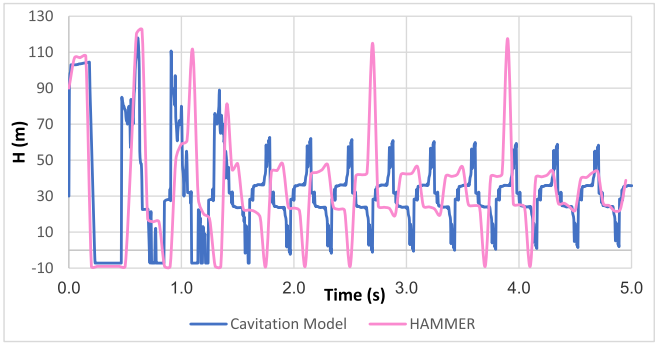

Fig. 6. Comparison between Hammer and Cavitation Model for the same lab conditions.

Table 2
Peak pressure, peak time and wave phase difference for the three different models.

Feature	Calibrated *HAMMER* model	Calibrated cavitation model
Head range (m)	−10 to 122	−8.5 to 120
Time to peak (s)	0.65	0.61
Wave Phase fit	Sufficient with spurious peaks	Very good
Behaviour	Sharp, with peaks not physically justified	Damped, smoother
Cavitation Handling	Likely with other interactions	Explicitly modelled
Suitability	Fast transient simulation and better friendly use	Cavitation-sensitive analysis

3.4.2. *Case studies and Parameter's definition*

A comprehensive approach to modelling hydrotransients with cavitation using machine learning (ML) techniques is presented. Hydrotransients are rapid changes in fluid flow within pipelines, often caused by operational shifts such as valve closures or pump failures. These transients can lead to pressure surges and drops, which in turn may trigger cavitation—a damaging phenomenon where vapour bubbles form and collapse violently inside the fluid system depending on the flow conditions. Traditional modelling of these events relies on solving complex partial differential equations, which are computationally intensive and require detailed knowledge of system parameters. To address these limitations, this research proposes a machine learning-based framework that digitises the solution space of hydrotransient models, allowing for fast and accurate predictions without the need for exhaustive simulations.

In this framework, ML algorithms are trained to predict key hydraulic responses – specifically, the maximum (Hmax) and minimum (Hmin) pressure heads – based on the selected input variables such as water flow rate (Q) and internal pipe diameter (D). The simulation setup includes a wide range of flow rates from 25 to 950 /h and pipe diameters from 0.005 to 0.06 m (Fig. 8) in a total of 32 series of case studies.

Among the tested models, a three-layered neural network demonstrates superior performance, achieving a R^2 of 0.86 for Hmax and 0.94 for Hmin during validation, and 0.46 and 0.91, respectively, during testing. These results indicate that the model is highly effective at capturing the dynamics of pressure fluctuations and cavitation risk.

The different pressure heads reveal that high Q values combined with small D values can lead to high velocities and pressure drops, increasing cavitation likelihood. The H dip coincides with high Q and low D, where the risk is even more pronounced leading to the cavitation can be expanded to the all pipe length, as seen in a sample most representative of 32 case studies, in Fig. 9, observing the Hmax continuous along the all pipe. Conversely, series with balanced Q/D ratios likely avoid cavitation.

The provided graphs illustrate the hydrotransient head variation over time at the downstream section and the pressure head envelope along the pipe length (L) for various flow rates (Q) and pipe diameters (D) conditions, highlighting the influence of these parameters on pressure fluctuations and cavitation risk. The comparison of the selected cases is summarised in Table 3.

The cases are categorised by their general flow rate (Q) and pipe diameter (D) conditions, which correlate with the resulting maximum (H max) and minimum (H min) pressure heads.

Regarding the general trend and cavitation risk: the key pattern observed across these cases is that the most extreme pressure heads (highest H max and lowest H min) occur in conditions combining high flow rate (Q) with small pipe diameter (D). Cavitation Likelihood is the risk of cavitation, where vapour bubbles form and collapse violently, which is strongly indicated by the minimum pressure head (H min). High Risk: Cases 1, 12, 22, and 31 show Hmin values attaining the vapour pressure, confirming the cavitation occurrence. On the other hand, the low risk of e.g. Cases 8 and 17, with more balanced Q/D ratios or a larger diameter, avoids the lowest pressure dips and consequently the cavitation risk.

Pressure Fluctuation at downstream Head Variation plots show that high Q/low D ratios lead to larger and more violent oscillations in pressure head over time, with the maximum pressure surges reaching up to ~400 m in Case 22. In the envelope shape, the H max envelope (maximum pressure along the pipe length, L) is continuous along the pipe in high cavitation risk scenarios (like Cases 22 and 31 from Fig. 7),

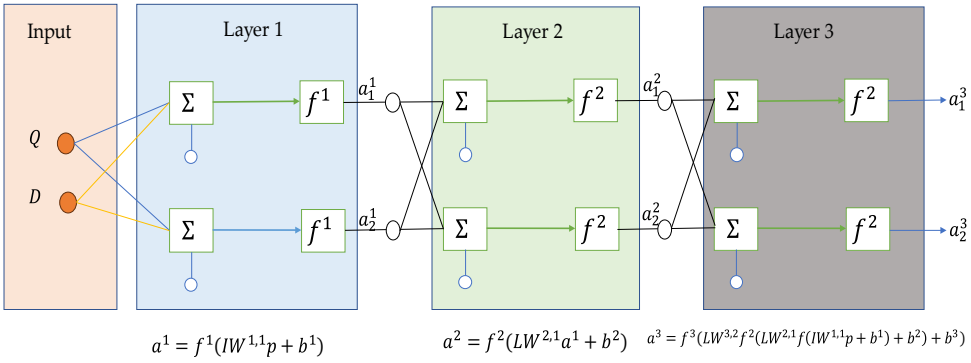

Fig. 7. Scheme of the three-layered neural network.

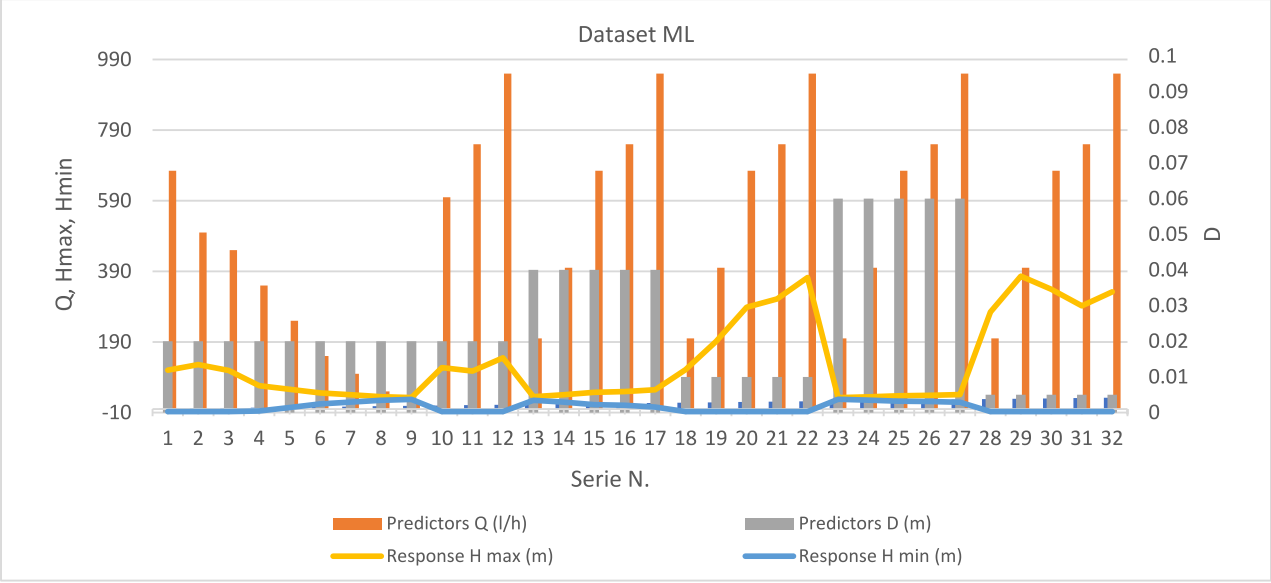

Fig. 8. Identification of experiments based on specific predictor variables towards extreme head responses.

indicating that the cavitation expands to the entire pipe length.

On the other hand, considering an air-valve installed in the middle of the pipe length, and because the pipe for the total length has a small increasing slope, it results in a non-efficiency of this protection device (Fig. 10) and in some conditions can be not recommended. The results are presented for some of the worst conditions, such as for example Cases 12 and 22.

The integration of air valves into hydraulic systems, particularly in the context of water hammer mitigation and cavitation control, demands careful consideration and judicious application. While air valves can serve to attenuate pressure surges and reduce vacuum conditions that promote cavitation, their improper placement or excessive use may inadvertently destabilise transient flow regimes, in particular for not significant ascending slope pipes. In certain configurations, they can introduce delayed air venting/release, amplify oscillatory behaviour, or even trigger secondary pressure peaks due to rapid air entrainment and expulsion. Therefore, their deployment should be guided by detailed transient analysis, supported by numerical modelling and experimental validation, to ensure that their influence enhances – rather than compromises – system resilience and operational safety.

3.4.3. ML application

The application of Machine Learning (ML) in this study provides a powerful, data-driven approach to modelling the complex hydraulic transients in pipeline systems, particularly focusing on the risk of cavitation. The motivation and predictive scope of the ML model is developed to address the limitations of traditional hydrotransient modelling. Modelling hydrotransient events—rapid changes in fluid flow caused by operational shifts like valve closures or pump failures—traditionally relies on solving complex partial differential equations. This process is computationally intensive and requires detailed knowledge of numerous system parameters. ML framework digitises the solution space of these hydraulic models, enabling fast and accurate predictions without requiring exhaustive, full-scale simulations. Regarding the predictive target, the ML algorithms were specifically trained to predict in this research two key hydraulic responses. The maximum (H max) in Fig. 11a by validation model, defining the model stage (Fig. 11b) using the Simulink model showed din Fig. 11c. The minimum (H min) pressure heads were shown in Fig. 12a by validation model, defining the model stage (Fig. 12b) and the Simulink model used (Fig. 12c). The role of Predictor Variables (Input Features), the model uses two physically grounded input features, water flow rate (Q) and internal pipe diameter (D), which directly influence wave propagation speed, pressure head amplitude, and cavitation susceptibility. The variable Flow Rate (Q) shows that Higher flow rates increase the fluid's kinetic energy, which can potentially amplify pressure surges and transient oscillations throughout the system. On the other hand, the pipe diameter (D) showed that smaller diameters intensify velocity gradients and frictional losses, which are the conditions that can exacerbate pressure drops and the onset of cavitation. For interpretability, a

sensitivity analysis is incorporated to quantify the relative influence of Q and D on H max and H min, which helps guide future feature selection. In terms of application results and practical implications, the model's high performance and reliable predictions offer significant benefits for system management and design.

Fig. 11 presents the comparison between true and predicted values of Hmax. Similarly, the three-layered neural networks were the best model for values of Hmin, with a coefficient of determination of 0.94 for

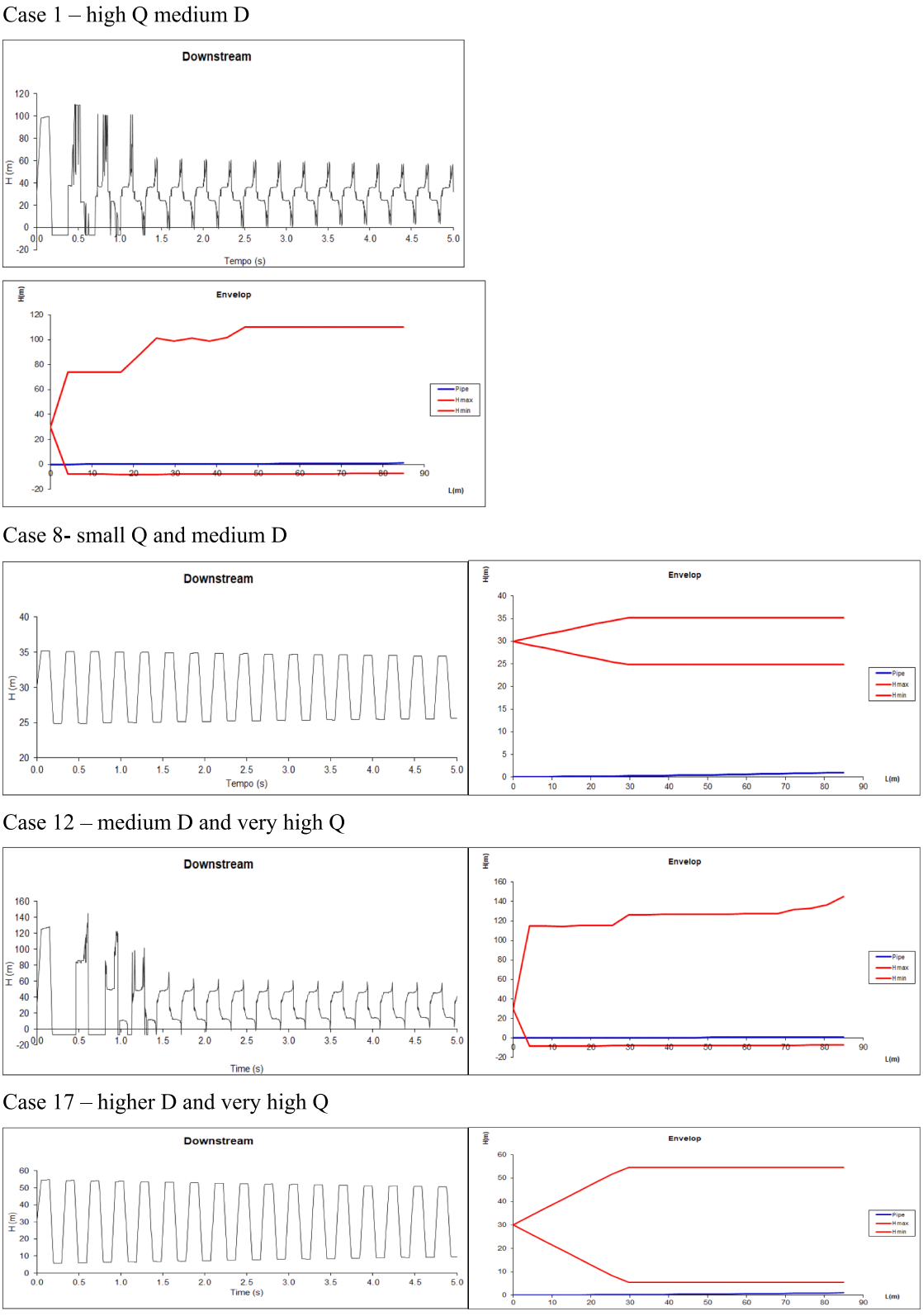

Fig. 9. Representatives of pressure oscillation with or not cavitation as function of Q and D: Cases 1, 8, 12, 17, 22 and 31.

Case 22 - small D and very high Q

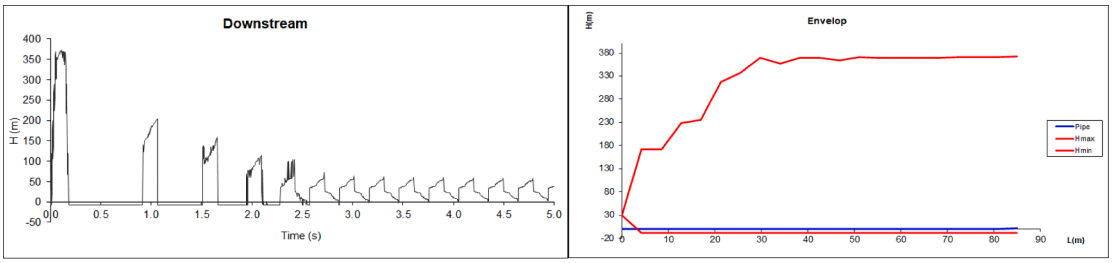

Case 31 – very small D and high Q

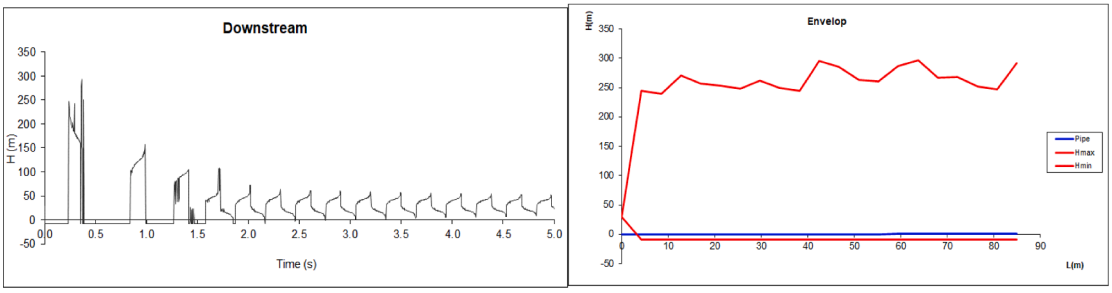

Fig. 9. (*continued*).

validation and testing stages (Fig. 12).

Comparisons between predicted and actual values further validate the model's accuracy, showing tight alignment across both validation and testing phases. The ability to reliably predict Hmin is particularly significant, as low-pressure conditions are closely associated with cavitation onset. By accurately forecasting these scenarios, the model enables proactive management of fluid systems, helping operators adjust flow rates or pipe configurations to mitigate cavitation risks. Additionally, the ML-based approach supports design optimisation, allowing engineers to simulate various operational conditions and select configurations that minimise the likelihood of cavitation without resorting to full-scale hydraulic modelling.

Overall, the integration of machine learning (ML) into hydro-transient modelling offers a powerful tool for enhancing operational safety, improving system design, and streamlining decision-making in fluid transport networks. The methodology demonstrates how data-driven techniques can complement traditional engineering approaches, providing fast, interpretable, and scalable solutions to complex hydraulic challenges.

Fig. 13 presents the analysis of Shapley importance for the predictors D and Q in the estimation of the responses (Hmax and Hmin in Fig. 13a and (b), respectively) considering the best preset (three-layered neural network). For both responses, the predictor D (internal pipe diameter) exerts a greater influence than Q on the model predictions, as its absolute contributions across all observations are consistently higher.

Table 4 presents the coefficient of determination for all machine learning presets, where the best fit was performed using the three-layered neural networks.

In total, 28 machine learning (ML) pre-sets, were used to fit the dataset of Hmax and Hmin. Results indicate that in both simulations, the three-layered neural network presented the best values of the coefficient of determination (R^2), the Root Mean Square Error (RMSE), and Mean Absolute Error (MAE). It implies that this pre-set can be used for making predictions. Table 4 presents a comparative analysis of 28 machine learning models applied to predict maximum (Hmax) and minimum (Hmin) pressure heads, using R^2, RMSE, and MAE scores for both validation and test datasets. The R^2 metric, ranging from 1 (perfect fit) to negative values (worse than a constant predictor), serves as a key

Table 3
Some representative case studies for different Q and D in the transition between no or cavitation events.

Case	Condition	Downstream Head Variation	Envelop along L (H vs L)	Observation
Case 8	Small Q & Medium D	Oscillations between ~ 25 m and ~ 35 m. Low amplitude and stable.	Narrow envelope (Hmax ~ 35 m, Hmin ~ 25 m).	Low pressure fluctuation and minimal cavitation risk (balanced Q/D ratio).
Case 17	Higher D & Very High Q	Oscillations between ~ 20 m and ~ 60 m. Regular, high amplitude.	Wide envelope (Hmax ~ 60 m, Hmin ~ 20 m).	Significant pressure fluctuation, but Hmin remains positive, suggesting no cavitation (higher D buffers the effect of very high Q).
Case 1	High Q & Medium D	Highly irregular, large pressure drops, and spikes, with some cycles reaching close to 0 m and others over 100 m.	Very wide envelope (Hmax ~ 120 m, Hmin ~ -20 m). Hmin is below zero head.	Severe pressure fluctuations and very likely cavitation due to Hmin dipping to negative values.
Case 12	Medium D & Very High Q	Irregular, very high peaks (~160 m) followed by large pressure drops (~0m).	Very wide envelope (Hmax ~ 140 m, Hmin is slightly above zero head). Hmin is close to the zero head.	Very high pressure surges (due to Very High Q) and a high risk of cavitation
Case 31	Very Small D & High Q	Initial very high peak (~350 m), followed by significant, irregular oscillations with high peaks and drops.	Very wide envelope (Hmax ~ 350 m, Hmin close to 0 m). Hmax continues to fluctuate significantly along the pipe.	Extremely high pressure surges and drops. Pronounced cavitation risk due to the combination of high Q and very small D, which generates high velocities and pressure drops.
Case 22	Small D & Very High Q	Initial extremely high peak (~400 m), then rapid, high-amplitude, and decaying oscillations.	Extremely wide envelope (Hmax ~ 400 m, Hmin slightly above 0 m). Hmax increases along the pipe.	The combination of very high Q and small D results in the highest pressure surge and a significant pressure drop, leading to an extremely high risk of cavitation.

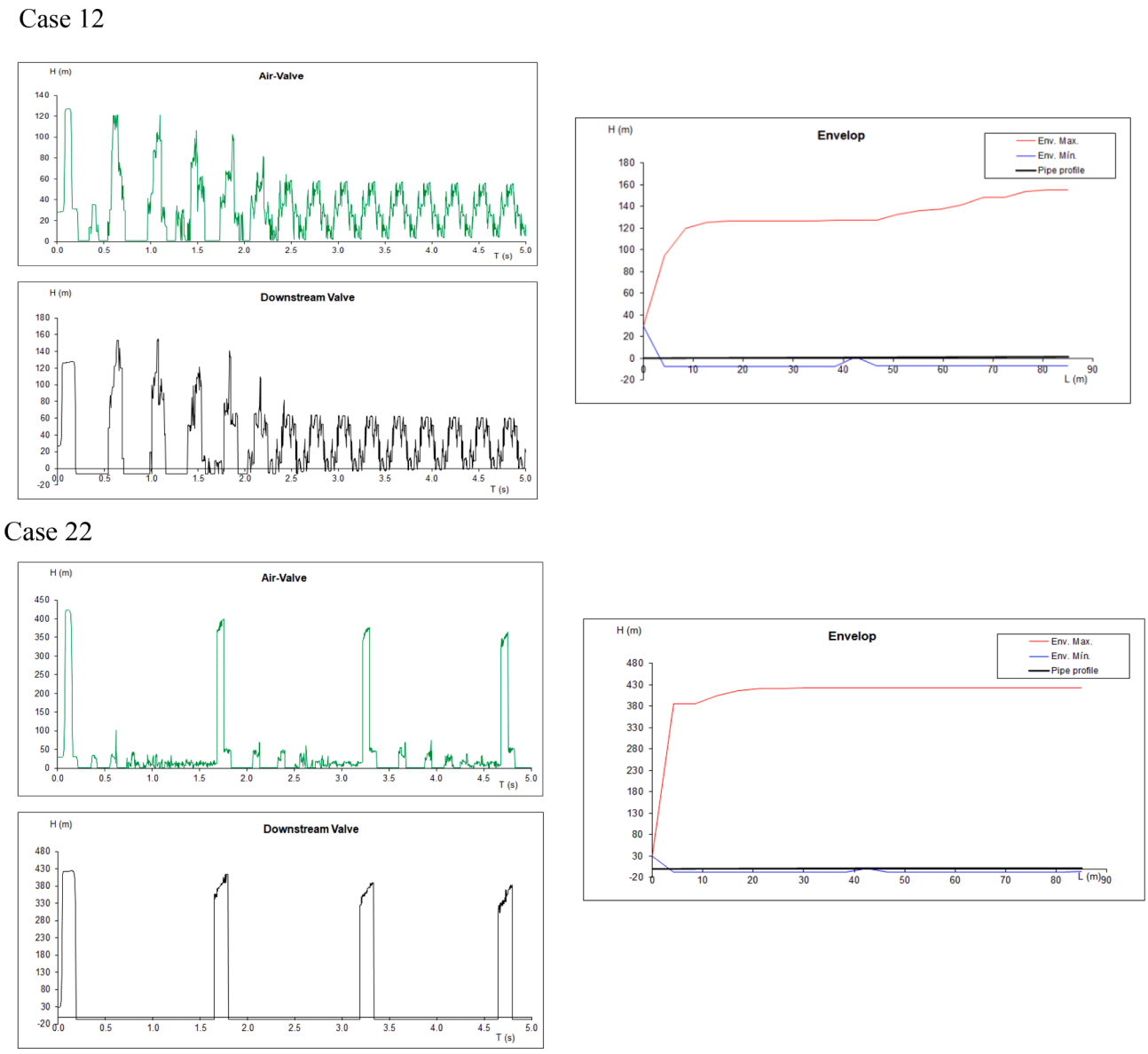

Fig. 10. Cases 12 and 22 with cavitation and air-valve installed in the middle of pipe length.

indicator of model performance and generalisation. Minimum values of RMSE and MAE indicate the best fit. Starting with tree-based models, Fine Tree shows high validation scores of R^2 for Hmax (0.60) but fails to generalise. Medium and Coarse Trees perform even worse, with zero validation scores and highly negative test scores, indicating model collapse or severe overfitting. Ensemble methods like Boosted and Bagged Trees offer slight improvements but still yield negative test R^2 values, suggesting limited utility for this task. Linear models, including standard, robust, stepwise, and interaction-based variants, demonstrate consistent validation performance for Hmin (around 0.83–0.84) and modest results for Hmax (0.57–0.66). However, their test scores for Hmax remain negative, while Hmin test scores hover near zero, indicating moderate generalisation. Among these, Robust Linear slightly outperforms others in test reliability. Support Vector Machines (SVMs) show varied behaviour. Linear SVM achieves decent validation scores but weak test performance. Quadratic and Cubic SVMs stand out, with Quadratic SVM reaching 0.84 (Hmax test) and Cubic SVM excelling in Hmin prediction (0.93 validation, 0.47 test). Gaussian SVMs are inconsistent: Medium Gaussian SVM performs well on Hmax validation (0.58) but poorly on Hmin test (−0.40), while Coarse and Fine variants struggle across the board. Gaussian Process Regression (GPR) models consistently deliver high validation scores for Hmin (0.98 across all variants). These models appear robust and well-suited for Hmin prediction, offering both accuracy and generalisation. Neural networks emerge as top performers, particularly for Hmin. The Bilayered Neural Network achieves near-perfect validation (0.99) and strong test performance (0.80), while the Three-layered Neural Network balances both Hmax and Hmin with test scores of 0.92 and 0.91, respectively. Medium and Wide networks also perform well, though Wide NN shows a drop in Hmax test accuracy. Finally, kernel-based models like SVM Kernel and Least Squares Regression Kernel show poor generalisation, with negative test scores across both targets. A similar analysis can be carried out using the RMSE and MAE, which shows that the three-layer neural network provides a good level of agreement for H_{max}. During the testing stage, RMSE and MAE values of 27.00 m and 17.11 m, respectively, were obtained—both of which are low compared with the values observed in Fig. 11.

In summary, the Three-layered Neural Network and Bilayered Neural Network provide the most reliable and generalizable predictions, especially for Hmin. GPR models offer robust alternatives with strong validation and acceptable test scores. Cubic and Quadratic SVMs are competitive, particularly for Hmin. Linear models are stable but limited

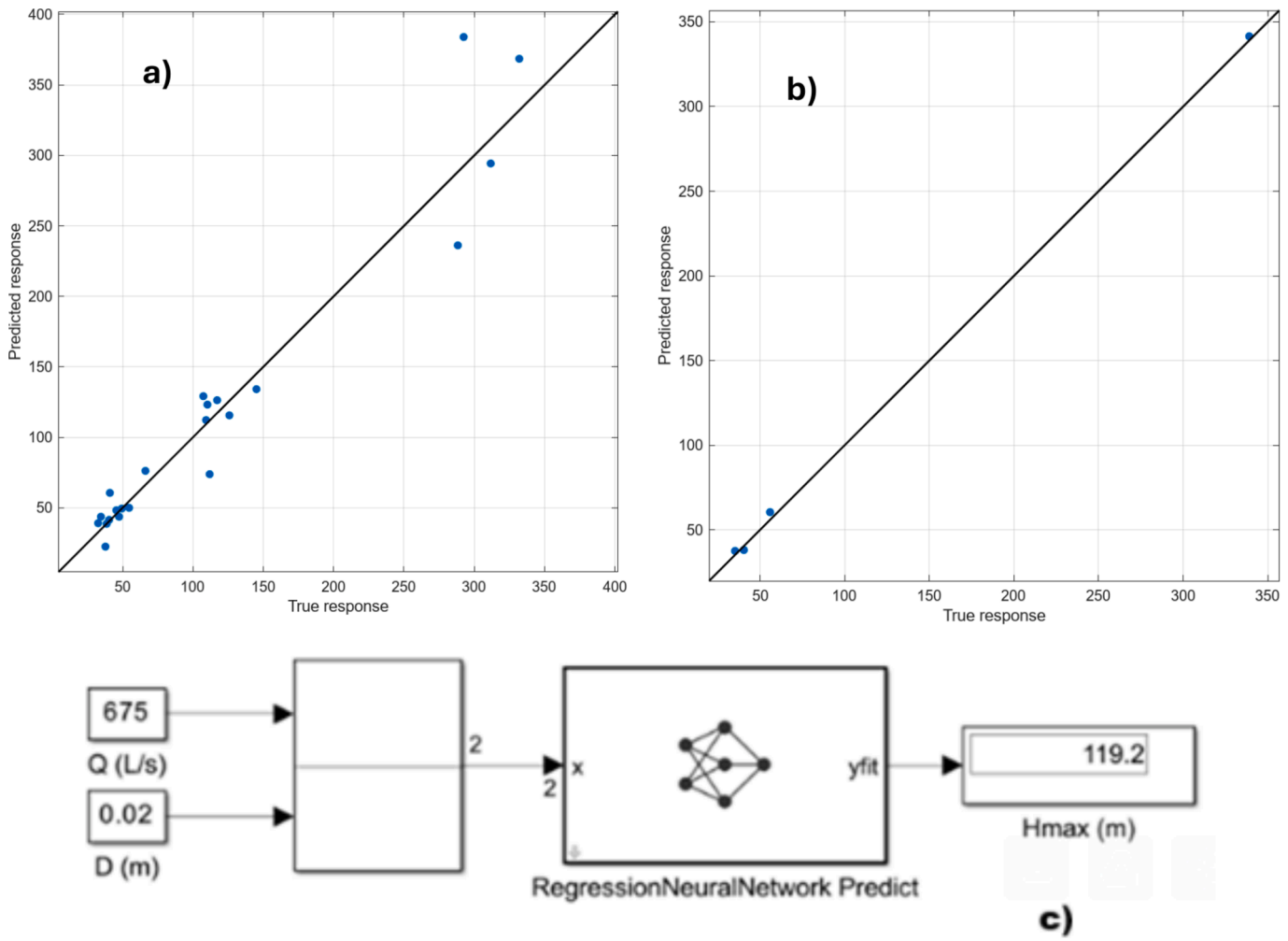

Fig. 11. True versus predicted Hmax: (a) validation stage; (b) testing stage; and (c) Simulink model.

in generalisation, while tree-based and kernel methods generally underperform. This analysis suggests that for hydrotransient modeling tasks involving pressure head prediction, deep neural architectures and GPR methods are the most promising.

Hence, cavitation mitigation relies on the ability to reliably predict H min, which is crucial, as low-pressure conditions are associated with cavitation onset. By accurately forecasting these scenarios, the model enables proactive management of fluid systems. Designers or Operators can adjust flow rates or pipe configurations to mitigate cavitation risks before they occur. In design Optimisation: The ML-based approach supports design optimisation, allowing engineers to rapidly simulate various operational conditions and select pipe configurations (e.g., specific Q and D combinations) that minimise the likelihood of cavitation without resorting to computationally expensive full-scale hydraulic modelling. In the overall significance, the integration of ML into hydrotransient modelling is deemed a powerful tool for enhancing operational safety, improving system design, and streamlining decision-making in fluid transport networks. This methodology demonstrates how data-driven techniques can complement traditional engineering approaches to provide fast, interpretable, and scalable solutions to complex hydraulic challenges.

4. Conclusions

A hydraulic transient Cavitation Model was developed to analyse system behaviour under cavitation effects across different flow rates and pipe diameters, combining a research model with full mathematical formulation and a commercial reference model (HAMMER, Bentley). An experimental set-up was used to calibrate parameters, focusing on fast downstream valve closure that induces sudden pressure surges and oscillations, where cavitation influences extreme pressure values. The methodology integrates classical hydraulics with machine learning, beginning with the Method of Characteristics (MOC) to discretise pipelines and apply governing equations of unsteady flow, while a specialised cavitation routine imposes vapour pressure conditions when pressure drops below the threshold. Simulation data from 32 case studies, covering flows between 25 and 950 l/h and diameters from 0.005 to 0.06 m, trained a three-layer neural network to predict maximum and minimum pressure heads based on flow rate and diameter, achieving high accuracy with coefficients of determination of 0.97 and 0.98 respectively. The approach highlights the importance of validated numerical modelling for safe integration of air valves in water hammer and cavitation control. Expanding the framework with machine learning introduces a transformative advance in hydrotransient modelling, reducing reliance on computationally intensive deterministic simulations, recognising nonlinear relationships between hydraulic variables and outcomes, and enabling scalable, adaptive, and interpretable predictive tools. This hybrid methodology supports proactive maintenance, virtual prototyping, and safer, more resilient fluid transport infrastructures. Ultimately, the fusion of physics-based hydraulics and ML-driven prediction establishes a powerful framework for accurate cavitation analysis, efficient management of transient phenomena, and sustainable design of hydraulic systems. Reliable prediction of the minimum pressure head (Hmin) is critical, as low-pressure conditions

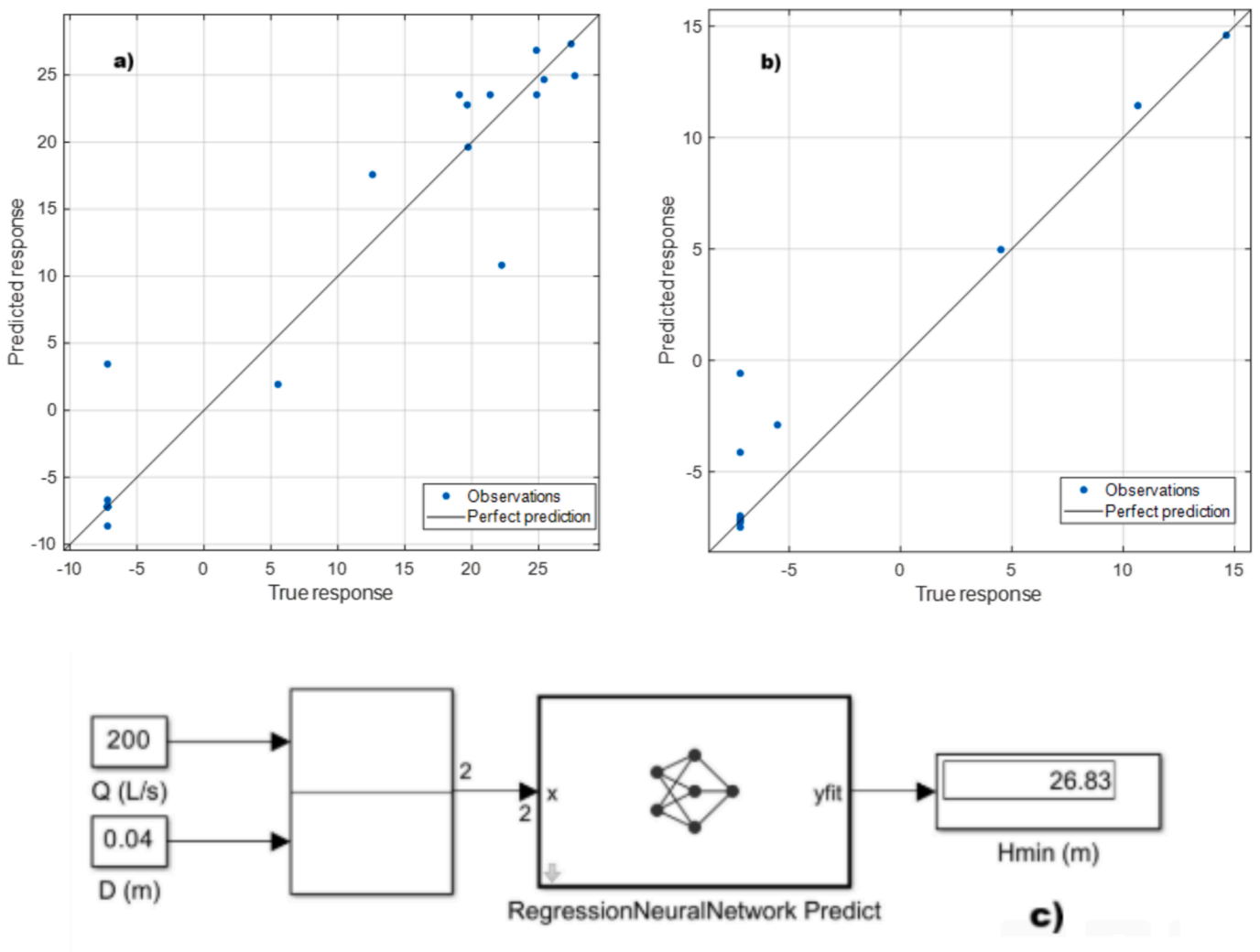

Fig. 12. True versus predicted Hmin: (a) validation stage; (b) testing stage; and (c) Simulink model.

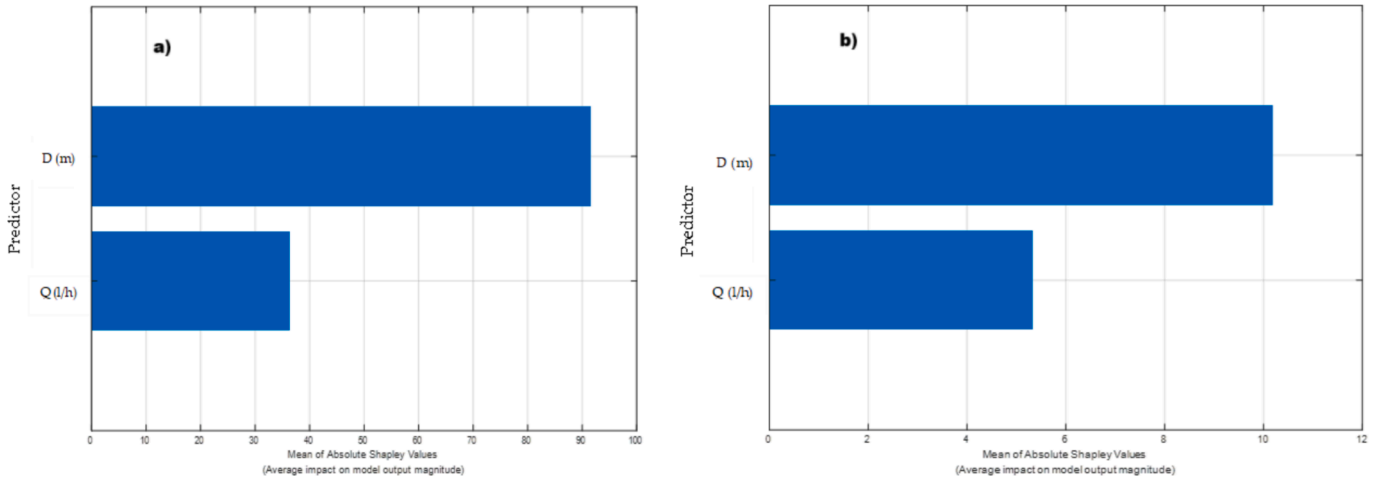

Fig. 13. Computation of Shapley values: (a) Hmax; and (b) Hmin.

Table 4
Computation of the coefficient of determination for all machine learning pre-sets.

Preset	Hmax						Hmin					
	R^2 (V)	R^2 (T)	RMSE (V)	RMSE (T)	MAE (V)	MAE (T)	R^2 (V)	R^2 (T)	RMSE (V)	RMSE (T)	MAE (V)	MAE (T)
Linear	0.66	0.77	57.78	57.54	49.03	44.50	0.83	−0.09	6.87	8.19	5.89	7.04
Interactions L	0.66	0.80	57.76	52.67	51.01	31.41	0.84	−0.72	6.58	10.32	5.63	8.56
Robust L	0.50	0.76	69.70	58.20	55.17	43.78	0.83	−0.06	6.94	8.09	5.93	6.95
Stepwise L	0.57	0.77	64.44	57.54	56.45	44.50	0.83	−0.09	6.87	8.19	5.89	7.04
Fine Tree	0.60	0.81	62.26	51.90	39.34	46.94	0.32	−1.97	13.66	13.54	10.20	9.65
Medium Tree	0.00	−0.01	98.49	120.06	74.16	103.75	0.00	−2.04	16.60	13.69	15.88	12.60
Coarse Tree	0.00	−0.01	98.49	120.06	74.16	103.75	0.00	−2.04	16.60	13.69	15.88	12.60
Linear SVM	0.55	0.53	65.96	81.76	45.79	53.85	0.80	0.03	7.45	7.72	5.95	6.60
Quadratic SVM	0.84	0.92	39.20	34.62	27.45	23.68	0.82	0.23	7.05	6.90	5.60	5.44
Cubic SVM	0.67	0.92	56.65	32.76	34.49	21.39	0.93	0.47	4.35	5.71	2.76	5.01
Fine G SVM	0.28	0.58	83.44	77.45	56.49	48.11	0.70	−2.11	9.03	13.86	7.67	12.11
Medium G SVM	0.58	0.79	63.59	54.22	42.05	29.78	0.96	−0.40	3.21	9.29	2.56	7.70
Coarse G SVM	0.33	0.35	80.36	96.39	50.67	69.88	0.72	−0.10	8.83	8.23	7.42	6.48
Efficient L LS	−0.01	0.34	99.11	96.75	77.03	53.12	0.07	−1.80	15.99	13.15	14.66	11.24
Efficient L SVM	0.06	0.17	95.27	108.74	71.09	73.34	−0.79	−0.93	22.18	10.92	20.58	10.32
Boosted Trees	−0.12	0.39	104.36	93.30	83.24	78.84	0.26	−0.19	14.24	8.57	12.68	7.07
Bagged Trees	0.09	0.34	93.88	96.88	76.56	81.45	0.29	−0.35	14.01	9.12	13.41	8.39
Squared E GPR	0.86	0.97	37.42	21.81	29.55	15.06	0.98	0.48	2.36	5.65	1.71	2.98
Matern 5/2 GPR	0.87	0.94	34.96	29.97	25.76	16.11	0.98	0.54	2.19	5.35	1.61	2.88
E GPR	0.88	0.97	34.30	22.19	23.34	12.20	0.98	0.25	2.29	6.81	1.70	5.11
RQ GPR	0.88	0.93	34.21	31.50	24.24	16.95	0.98	0.53	2.27	5.41	1.72	2.83
Narrow NN	0.64	0.98	58.81	17.84	36.39	12.70	0.88	0.49	5.81	5.61	2.48	2.55
Medium NN	0.49	0.98	70.68	17.71	39.96	12.43	0.95	0.30	3.57	6.59	2.22	3.20
Wide NN	0.53	0.93	67.75	31.25	36.24	18.83	0.97	0.36	2.83	6.28	1.63	3.16
Bilayered NN	0.08	0.93	94.59	31.33	47.07	14.39	0.99	0.80	1.92	3.52	0.96	1.84
Trilayered NN	0.92	1.00	27.00	2.92	17.11	2.78	0.94	0.91	3.98	2.35	2.35	1.29
SVM Kernel	−0.05	−0.02	101.05	120.51	70.57	76.33	−0.24	−2.51	18.46	14.73	17.20	13.18
LS R Kernel	0.59	0.85	63.43	46.15	47.83	32.52	0.84	−0.41	6.67	9.32	5.94	7.79

being V = Validation, T = Test, L = Linear, G = Gaussian, LS = Least Square, E = Exponential, RQ = Rational Quadratic, SVM = Support Vector Machine, GPR = Gaussian Process Regression, NN = Neural Network, and R = Regression.

directly trigger cavitation, a damaging phenomenon in pipelines. By forecasting these scenarios, the machine learning (ML) model enables proactive system management, allowing operators and designers to adjust flow rates or pipe configurations to mitigate risks before they occur. This data-driven approach also supports design optimisation, offering rapid simulation of operational conditions and selection of configurations that minimise cavitation without the computational burden of full-scale hydraulic modelling. The integration of ML into hydrotransient analysis thus enhances safety, improves design efficiency, and streamlines decision-making. Comparative evaluation of 28 ML models shows that tree-based and kernel methods generally underperform, while linear models achieve moderate generalisation, particularly for Hmin. Support Vector Machines with nonlinear kernels perform better, and Gaussian Process Regression yields consistently strong validation scores. Neural networks, especially three-layered and bilayered architectures, prove the most reliable and generalisable predictors across both maximum and minimum pressure targets. Uncertainty is addressed through experimental calibration of the cavitation model and systematic validation of the machine-learning surrogate across a wide range of flow rates and pipe diameters. This combined approach quantifies variability in extreme pressure predictions and ensures robust and reliable estimation of cavitation-related pressure limits.

DT operates by aligning model outputs with experimental baselines, and by using machine learning to extend predictions to scenarios that cannot be physically replicated in the laboratory. Thus, the DT framework here included: (i) Modelling prediction: Numerical cavitation modelling and ML-based surrogate modelling. (ii) Real-time measurements: Laboratory tests serving as the physical counterpart for calibration and validation. (iii) Data interaction: Continuous comparison and adjustment between model outputs and experimental baselines. Overall, this methodology demonstrates how ML can complement traditional engineering approaches, delivering fast, interpretable, and scalable solutions to complex hydraulic challenges. The work addresses limitations in existing methods by bridging deterministic hydraulic modelling, commercial black-box tools, and purely data-driven approaches. Classical methods such as the Method of Characteristics (MOC) are reliable but limited in representing cavitation, as commercial software often conceals formulations and restricts parameter definition. Our tailored cavitation model overcomes this by explicitly formulating governing equations, boundary conditions, and vapour cavity occurrence, enabling reproducible and adaptable analysis. A further limitation in the literature is the lack of experimental grounding; many studies rely only on numerical validation. This gap is addressed through a dedicated laboratory set-up, where controlled transients and measured oscillations calibrate the cavitation model, ensuring that the framework reflects real-world behaviour. While this study does not yet test different pipe materials or real field conditions (e.g., temperature variation, pipe elasticity, pipe profiles, air valve behaviour), it advances beyond existing methods by coupling deterministic modelling, experimental calibration, and predictive analytics, thereby improving transparency, reproducibility, and predictive capability in hydraulic transient analysis. An explicit limitation and clarification for future work may involve coupling the 1D approach with CFD and experimental campaigns to capture localized three-dimensional effects.

5. Declaration of generative AI and AI-assisted technologies in the manuscript preparation process

AI technologies were used to use of basic tools, such as tools used to check grammar, spelling and references.

CRediT authorship contribution statement

Oscar E. Coronado-Hernández: Investigation, Conceptualization, Data curation, Formal analysis, Resources, Supervision, Writing – review & editing. **Duban A. Paternica-Verona:** Methodology, Conceptualization, Data curation, Formal analysis, Writing – original draft. **Modesto Pérez-Sánchez:** Writing – original draft, Methodology,

Conceptualization, Data curation, Formal analysis, Investigation, Resources, Visualization. **Dídia I.C. Covas:** Writing – review & editing, Visualization, Resources, Data curation, Formal analysis, Conceptualization, Supervision. **Helena M. Ramos:** Writing – original draft, Supervision, Methodology, Investigation, Funding acquisition, Data curation, Conceptualization, Formal analysis, Project administration, Resources.

Funding

Funding for open access charge: CRUE-Universitat Politècnica de València.

Declaration of competing interest

The authors declare that they have no known competing financial interests or personal relationships that could have appeared to influence the work reported in this paper.

Acknowledgments

This work was supported by FCT, UID/6438/2025 CERIS, in the Hydraulic Laboratory, for experiments on pumped storage performance, and the project HY4RES (Hybrid Solutions for Renewable Energy Systems) EAPA_0001/2022 from the INTERREG ATLANTIC AREA PROGRAMME.

Data availability

Data will be made available on request.

References

[1] A. Bergant, A.R. Simpson, A.S. Tijsseling, Water hammer with column separation: a historical review, J. Fluids Struct. 22 (2) (Feb. 2006) 135–171, https://doi.org/10.1016/j.jfluidstructs.2005.08.008.

[2] K. Urbanowicz, A. Bergant, A. Kodura, M. Kubrak, A. Malesińska, P. Bury, M. Stosiak, Modeling transient pipe flow in plastic pipes with modified discrete bubble cavitation model, Energies 14 (20) (2021) 6756, https://doi.org/10.3390/en14206756.

[3] H. Ramos, D. Covas, A. Borga, D. Loureiro, Surge damping analysis in pipe systems: modelling and experiments, J. Hydraul. Res. 42 (2004) 413–425, https://doi.org/10.1080/00221686.2004.9641209.

[4] S. Cheng, C. Liu, Y. Guo, R. Arcucci, Efficient deep data assimilation with sparse observations and time-varying sensors, J. Comput. Phys. 496 (2024) 112581, https://doi.org/10.1016/j.jcp.2023.112581.

[5] J. Lo Presti, C. Giudicianni, C. Toffanin, E. Creaco, L. Magni, G. Galuppini, Combining clustering and regularised neural network for burst detection and localization and flow/pressure sensor placement in water distribution networks, Journal of Water Process Engineering, Volume 63, 2024, 105473, ISSN 2214-7144, https://doi.org/10.1016/j.jwpe.2024.105473.

[6] X. Li, C. Hu, H. Liu, X. Shi, J. Peng, An improved deep learning model for sparse reconstruction of cavitation flow fields, Phys. Fluids 36 (7) (2024) 077145, https://doi.org/10.1063/5.0216945.

[7] H.M. Ramos, V.S. Fuertes-Miquel, E. Tasca, O.E. Coronado-Hernández, M. Besharat, L. Zhou, B. Karney, Concerning dynamic effects in pipe systems with two-phase flows: pressure surges, cavitation, and ventilation, Water 14 (2022) 2376, https://doi.org/10.3390/w14152376.

[8] K. Urbanowicz, A. Bergant, M. Stosiak, A. Deptuła, M. Karpenko, M. Kubrak, A. Kodura, Water hammer simulation using simplified convolution-based unsteady friction model, Water 14 (19) (2022) 3151, https://doi.org/10.3390/w14193151.

[9] D.A. Paternina-Verona, O.E. Coronado-Hernández, M. Pérez-Sánchez, H.M. Ramos, Real-time analysis and digital twin modeling for CFD-based air valve control during filling procedures, Water (switzerland) 16 (2024), https://doi.org/10.3390/w16213015.

[10] Z. Tong, H. Liu, X.E. Cao, D. Westerdahld, X. Jin, Cavitation diagnosis for water distribution pumps: an early-stage approach combing vibration signal-based neural network with high-speed photography, Sustainable Energy Technol. Assess. 55 (2023) 102919, https://doi.org/10.1016/J.SETA.2022.102919.

[11] L. Ramezani, B. Karney, A. Malekpour, The challenge of air valves: a selective critical literature review, J. Water Resour. Plan. Manag. 141 (2015) 4015017, https://doi.org/10.1061/(ASCE)WR.1943-5452.0000530.

[12] L. Ramezani, B. Karney, A. Malekpour, Encouraging effective air management in water pipelines: a critical review, J. Water Resour. Plan. Manag. 142 (2016) 4016055, https://doi.org/10.1061/(ASCE)WR.1943-5452.0000695.

[13] L. Zhou, Y. Lu, B. Karney, G. Wu, A. Elong, K. Huang, Energy dissipation in a rapid filling vertical pipe with trapped air, J. Hydraul. Res. 61 (2023) 120–132, https://doi.org/10.1080/00221686.2022.2132309.

[14] P.D. Tran, Pressure transients caused by air-valve closure while filling pipelines, J. Hydraul. Eng. 143 (2017) 4016082, https://doi.org/10.1061/(ASCE)HY.1943-7900.0001245.

[15] American Water Works Association (AWWA) Air-Release, Air/Vacuum, and Combination Air Valves: M51; American Water Works Association, 2001; Vol. 51; ISBN 1583211527.

[16] B.E. Zechman, S.M. Ehsan, X. Lu, W. Jason, Digital twins for water distribution systems, J. Water Resour. Plan. Manag. 149 (2023) 02523001, https://doi.org/10.1061/JWRMD5.WRENG-5786.

[17] Elias Tasca, Bryan Karney, Mohsen Besharat, Helena Ramos, Ling Zhou, Insights and Challenges Associated with Air in Pressurized Water Conveyance Systems, June 2022, Conference: World Environmental and Water Resources Congress 2022 HTTPS://DOI.ORG/10.1061/9780784484258.098.

[18] Bahrami Chegeni, I.; Riyahi, M.M.; Bakhshipour, A.E.; Azizipour, M.; Haghighi, A. Developing Machine Learning Models for Optimal Design of Water Distribution Networks Using Graph Theory-Based Features. Water 2025, Vol. 17, Page 1654 2025, 17, 1654, https://doi.org/10.3390/W17111654.

[19] Yang, X.; Zhu, J.; Zhang, Y.; Chen, B.; Tang, Y.; Jiang, R.; Kan, K.; Ye, C.; Zheng, Y. Study on the Cavitation Performance in the Impeller Region of a Mixed-Flow Pump Under Different Flow Rates. Water 2024, Vol. 16, Page 3195 2024, 16, 3195, https://doi.org/10.3390/W16223195.

[20] Chen, Y. System Simulation Techniques with MATLAB and Simulink; John Wiley & Sons, 2013; ISBN 1118694376.